Dominance of Atomic States in a Solid: Selective Breakdown of the Virtual Crystal Approximation in a Semiconductor Alloy, $Hg_{1-x}Cd_xTe$

W. E. Spicer, J. A. Silberman, J. Morgen,[a] and I. Lindau
Stanford Electronics Laboratory, Stanford University, Stanford, California 94305

and

J. A. Wilson
Santa Barbara Research Center, Goleta, California 93017

and

An-Ban Chen
Physics Department, Auburn University, Auburn, Alabama 36830

and

A. Sher
SRI International, Menlo Park, California 94025

(Received 4 May 1982)

Ultraviolet-photoelectron-spectroscopy experiments and a coherent-potential-approximation calculation of the density of states of $Hg_{1-x}Cd_xTe$ show a clear deviation from virtual crystal behavior in bands $\simeq 5$ eV below the valence-band maximum where there is a 60% s-electron contribution. The large ($\simeq 1.4$ eV) atomic s-state shift between Hg and Cd is responsible for this deviation, as well as for the decrease of the band gap (1.5 to 0 eV) with composition, the high electron mobility (10^6 cm^2/V s), and difficulties experienced with growth and mechanical properties.

PACS numbers: 71.25.Tn, 79.60.Eq

Over ten years ago, it was firmly established[1] that metallic alloys such as NiCu required consideration of markedly different potentials for each atomic species. This forced the abandonment of the rigid-band model for metallic alloys (which had been widely accepted up to that time) and had enormous significance for fields extending from metallurgy to catalysis. In contrast, the relatively simple virtual crystal approximation (VCA), in which average potentials are assigned to each sublattice site, had been successful with semiconductors.

The objectives of this paper are to (1) show definitive experimental and theoretical evidence for the selective breakdown of VCA in a semiconductor alloy ($Hg_{1-x}Cd_xTe$), (2) establish that the coherent-potential approximation (CPA) works well where VCA fails, and (3) explain the physics underlying the shortcomings of the VCA in terms of the atomic orbitals involved.

$Hg_{1-x}Cd_xTe$ exhibits a number of properties that are both of fundamental interest and suitable for exploitation.[2] Because the lattice constants of HgTe and CdTe are nearly identical, the entire composition range can be made in the zinc-blend structure with a continuous change of band gap from 1.5 eV (CdTe) to 0, making these materials prime candidates for use in infrared photodetectors. Enormous electron mobilities ($>10^6$ cm^2/V s) are found for small band gaps, confirming the occurrence of extremely nonlocalized wave functions near the band edges.[3] As we will see, the breakdown of VCA occurs deep in the valence bands, where the states are more localized and have a large atomic "s" character.

Ultraviolet-photoelectron-spectroscopy measurements were made on samples cleaved along a (110) face in ultrahigh vacuum ($p < 10^{-10}$ Torr) with photon energies ranging from 7 to 30 eV on four compositions, $x = 0.2$, 0.31, 0.39, and 1. Figure 1 shows energy distribution curves (EDC's) for $12 \leq h\nu \leq 17$ eV (resolution < 0.2 eV) for an alloy sample and CdTe. The valence-band maximum (VBM) is taken as the zero of energy. Two major groups of valence-band features appear between -3.5 and 0 eV, and one between -6 and -4 eV. The upper feature exhibits dispersion characteristic of delocalized states.[4] The lower feature shows no dispersion (as would be expected for a more localized state), and it is here that breakdown of VCA is found. This same qualitative valence-band behavior was found in all $Hg_{1-x}Cd_xTe$ samples.

In Fig. 2, we examine the experimental struc-

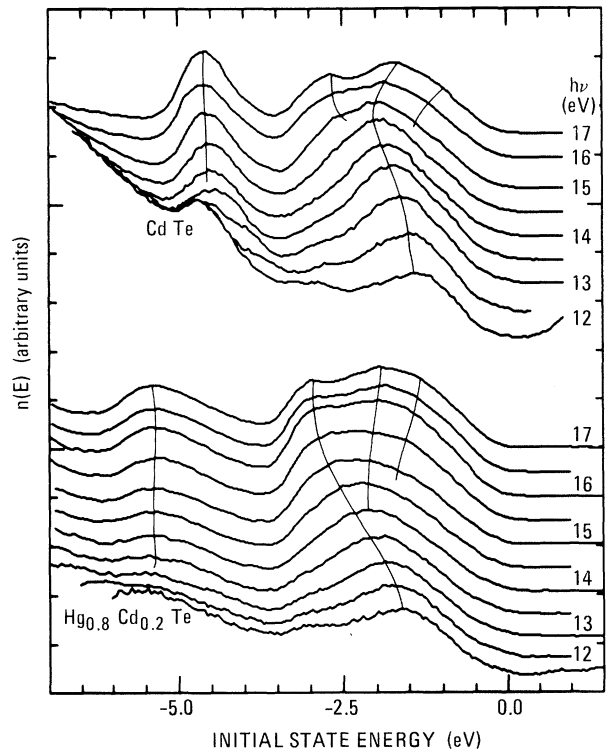

FIG. 1. Photoemission energy distribution curves for CdTe and the alloy $Hg_{0.8}Cd_{0.2}Te$. The number of electrons detected is plotted vs initial state energy with the origin set to the valence-band maximum. Contrast the relatively large dispersion and widths of the "p-like" bands within 3.5 eV of the valence-band maximum (VBM) with the small dispersion of the band centered about 5 eV below VBM. This band is relatively narrow in CdTe but broadened by the alloy effects in $Hg_{1-x}Cd_xTe$.

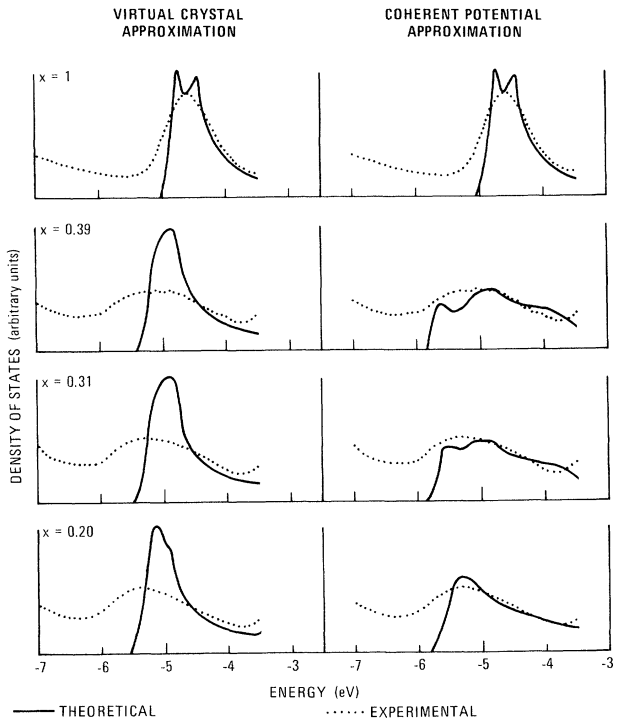

FIG. 2. Comparison of theory and experiment for $Hg_{1-x}Cd_xTe$ for the compositions indicated by the value of x in the figures. The virtual crystal approximation clearly does not agree with experiment for the alloys, whereas the agreement with coherent-potential theory is surprisingly good. No "experimental" broadening has been included in the theoretical curves, nor has background been subtracted from the experimental curves.

ture between -3.5 and -7 eV as a function of composition and compare it with the VCA and CPA calculations. The calculations give the density of states (DOS); because we found negligible dispersion for the features in this energy range, the EDC's should be closely related to the calculated DOS and can legitimately be compared. The experimental and theoretical curves were aligned in energy by superimposing the leading edge of the EDC's (i.e., experimental VBM) with the VBM given by the calculations. The structure in the calculated curves is sharp in comparison with the experimental curves. This results (at least in part) from the fact that no broadening has been put into the calculations to account for the finite (<0.2 eV) experimental resolution or other broadening effects. Furthermore, the low-energy scattering-induced tail in the EDC has not been subtracted from the data.

Figure 2 shows that the general experimental features and trends in the alloys are predicted well by the CPA, but not by the VCA: The VCA predicts a peak with a relatively narrow total width ($\simeq 0.5$ eV), which moves monotonically in energy from CdTe (-4.6 eV—weighted average of the doublet) to that calculated for HgTe (-5.5 eV—not shown in curves, because no experimental data were available for HgTe). Most importantly, the width of the VCA-predicted peak(s) does not increase appreciably with energy. The CPA results (in agreement with experiment) increase in width as one moves from CdTe into the alloys. For $x = 0.39$ eV, both experiment and CPA give a width of $\simeq 2$ eV, roughly four times what would be predicted by VCA. More detailed examination of the $x = 0.39$ and $x = 0.31$ CPA curves indicates that peaks can be resolved near -5.6 and -5.0 eV and that there exists a weaker shoulder near -4.2 eV. CPA calculations identify the origins of these three features: The

– 5.6-eV peak and the shoulder are due to Hg- and Cd-derived s states, respectively; the intermediate peak is a "VCA-like" peak with p symmetry. Note that it lies at the same energy as the VCA peak (left panel of Fig. 2) and, insofar as can be seen, moves with energy, as does the VCA peak.

The theory proceeds in three steps: obtaining accurate band structures for HgTe and CdTe, characterizing the disorder of the potential in the alloys, and executing the CPA calculation.[5] The Hamiltonian matrix $H_0(\vec{k})$ for a given $\vec{k}$ is calculated in the manner described in Ref. 5 with use of published[6] local empirical pseudopotentials. A systematic orthogonalization and $\vec{k}$-integration procedure transforms the initial Gaussian orbital sp^3 set into a set of completely orthonormal atomiclike orbitals (OAO). The diagonalization of $H(\vec{k})$ then yields a band structure without the spin-orbit splittings. The spin-orbit interaction is incorporated as a simplified Animalu model.[7] The other relativistic corrections (the velocity term and the Darwin term) do not alter the symmetry of $H(\vec{k})$ and are partially taken into account in $H(\vec{k})$ by the choice of the parameters in the empirical pseudopotential.

Because of the limitations of local pseudopotentials and the truncated basis set, the net Hamiltonian $H(\vec{k})+H_{so}(\vec{k})$ introduced thus far yields results differing from experiment by $\simeq 5\%$. The corrections needed to reach agreement with experiment are incorporated into the theory (as justified previously) by the addition of a localized perturbation Hamiltonian H_1.[5]

To facilitate the characterization of the local interactions and the CPA calculation, the OAO set is next transformed into completely orthonormal cell orbitals (OCO) with proper symmetries. The minimum basis then consists of two A_1 and six T_2 OCO's. When spin is included, each A_1 becomes two Γ_6 OCO's, and the six T_2's become four Γ_7 and eight Γ_8 OCO's. The crystal Hamiltonian matrix in the OCO basis for a given cell becomes block diagonal into eight 2×2 matrices: two in Γ_6, two in Γ_7, and four in Γ_8 representations. Because all the 2×2 matrices for a given representation are the same, there are only nine independent single-cell interactions: six diagonal energies $\epsilon_\alpha(\Gamma_\eta)$, $\alpha=1,2$, $\eta=6,7,8$; and three off-diagonal interactions γ_η. These local energy parameters for HgTe and CdTe have been determined from parametrized band structures; their values are listed in Table I. Note that major differences between HgTe and CdTe are in the $\epsilon_1(\Gamma_6)$ and γ_6 terms; these terms are influenced strongly by the $5s^2$ and $6s^2$ valence orbitals of Cd and Hg, respectively. (The physical significance of this is discussed below.) The antibonding $\epsilon_2(\Gamma_6)$ and all the other states (which have T_2 or p-like symmetry) have small energy differences.

TABLE I. Intracell Hamiltonian matrix elements for HgTe and CdTe.

Local energy parameter	Intracell Hamiltonian matrix element (eV) HgTe	CdTe
$\epsilon_1(\Gamma_6)$	−12.96	−11.19
$\epsilon_2(\Gamma_6)$	−2.26	−2.27
γ_6	−2.52	−4.31
$\epsilon_1(\Gamma_7)$	−7.16	−6.58
$\epsilon_2(\Gamma_7)$	−1.45	−1.45
γ_7	−3.59	−3.43
$\epsilon_1(\Gamma_8)$	−7.08	−6.55
$\epsilon_2(\Gamma_8)$	−1.42	−1.43
γ_8	−3.61	−3.43

In the OCO basis, the alloy Hamiltonian can be written as $H=\overline{H}+\sum_l V_l$, where $\overline{H}$ is the average periodic VCA Hamiltonian and the random part V_l is the sum over nine terms of the form $|\psi_l{}^\alpha\rangle \times \delta\epsilon_{\alpha\beta}\langle\psi_l{}^\beta|$, where the $|\psi_l{}^\alpha\rangle$ are the OCO's of the lth cell, and $\delta\epsilon_{\alpha\beta}$ are the deviations from the mean for the nine intercell interactions. If only the diagonal terms in V_l are retained, then the CPA calculation reduces to the one reported before.[5]

Why has VCA worked so well in other semiconductors but performed poorly with $Hg_{1-x}Cd_xTe$? First, note that $Hg_{1-x}Cd_xTe$ is the first "covalent" semiconductor alloy studied containing "light" ($Z<57$) and heavy ($Z>78$) atoms. The explanation lies in the atomic orbitals of these atoms. The relative binding energies of the p and s orbitals of the cations in covalent semiconductors do not change appreciably as one moves through the periodic table until one moves from atomic numbers below 57 to those above 78. Above $Z=78$, the s orbitals become markedly more tightly bound with respect to the p (or other higher-angular-momentum orbitals) as relativistic terms (which tend to decrease the orbital radius) become important. This is because the valence s orbitals, which penetrate the nucleus much more than do the orbitals with nonzero angular momentum, are more sensitive to these terms. We shall refer to this effect as the *s shift*. In the

present case, the ionization energy of the Hg $6s^2$ valence electrons is 1.4 eV higher than that of the Cd $5s^2$. It should further be noted that the work in the early 1960's showed[2] that both the decrease of E_g to zero and the high electron mobilities are associated with the metal s states of the conduction band decreasing in energy with increasing Hg content until they mix with the p states to form the valence-band maximum. We thus identify three phenomena (the breakdown of VCA, E_g going to zero, and high electron mobility) as resulting from the Hg $6s^2$ atomic levels being significantly below the Cd $5s^2$ levels.

$Hg_{1-x}Cd_xTe$ is perhaps the most promising material available for photodetection throughout the infrared, yet it has not been widely exploited. This may be because of difficulties in growing and handling the material[2]; we suggest that this also results from the "s shift" (i.e., selectivity increasing the bonding energy of the Hg valence s levels, which weakens the Hg-Te bond and leads to the difficulties mentioned above).

It is our hope that this paper will stimulate work to test our suggestions. Such work is greatly needed, both for fundamental understanding and to guide (and reduce the cost of) practical work.

This work was supported by U. S. Defense Advanced Research Projects Agency Contract No. MDA 903-80-C496 and U. S. Air Force Office of Scientific Research Contract No. F49620-81-K0012; work was performed at the Stanford Synchrotron Radiation Laboratory, which is supported by the National Science Foundation in cooperation with the U. S. Department of Defense. One of us (J.A.S.) was the recipient of a National Science Foundation predoctoral fellowship.

[a]Permanent address: Fysisk Institut, Odense University, Capusvej 55, DK-5230, Odense M, Denmark.

[1]See, for example, *Band Structure Spectroscopy of Metal and Alloys*, edited by D. J. Fabian and L. M. Watson (Academic, London, 1973).

[2]See, for example, R. Dornhaus and G. Nimtz, in *Solid-State Physics*, Springer Tracts in Modern Physics Vol. 78 (Springer-Verlag, Berlin, 1976), p. 1 and references therein.

[3]P. Morgen, J. Silberman, I. Lindau, W. E. Spicer, and J. A. Wilson, J. Cryst. Growth 56, 493 (1982); P. Pianetta, I. Lindau, C. M. Garner, and W. E. Spicer, Phys. Rev. B 18, 2792 (1978); P. Pianetta, I. Lindau, P. E. Gregory, C. M. Garner, and W. E. Spicer, Surf. Sci. 72, 298 (1978).

[4]J. A. Silberman, P. Morgen, I. Lindau, W. E. Spicer, and J. A. Wilson, to be published; W. E. Spicer, in *Optical Properties of Solids —New Developments*, edited by B. O. Seraphin (North-Holland, Amsterdam, 1976).

[5]A.-B. Chen and A. Sher, Phys. Rev. B 23, 5360 (1981).

[6]D. J. Chadi, J. P. Walter, and M. L. Cohen, Phys. Rev. B 5, 3058 (1972).

[7]A. O. E. Animalu, Philos. Mag. 13, 53 (1966).

One-Dimensional Localization and Interaction Effects in Narrow (0.1-μm) Silicon Inversion Layers

W. J. Skocpol, L. D. Jackel, E. L. Hu, R. E. Howard, and L. A. Fetter

Bell Laboratories, Holmdel, New Jersey 07733

(Received 1 March 1982)

The conductance of narrow (0.1-μm) silicon inversion layers has been measured at low temperatures. A divergent, nonmetallic decrease of conductance is observed below 30 K, in excellent quantitative agreement with the combined theories of weak localization and interaction effects in their one-dimensional form, if one assumes parameters comparable to those observed in wide (two-dimensional) inversion layers. In this novel experimental system both localization and interaction effects are present and comparable in size.

PACS numbers: 71.55.Jv, 72.15.-v, 73.40.Qv

Narrow [quasi one-dimensional (1D)] metal wires become nonmetallic at low temperatures.[1] The decrease of conduction is proportional to $e^2/\hbar$ and appropriate electron diffusion lengths, according to theory,[2] whenever these lengths exceed the transverse wire dimensions (the